Proceeding of the IEEE
International Conference on Robotics and Biomimetics
Dali, China, December 2019

Minimum Energy Consumption Braking Torque Distribution Scheme Based on STA Second-Order Sliding Mode Controller

Zhidong Huang, Guoqing Xu*
School of Mechatronics Engineering and Automation, Shanghai University
Shanghai 200444, China
gqxu@shu.edu.cn

***Abstract* - A four-wheel-drive electric vehicle has a regenerative braking function, and its braking stability changes while recovering part of the braking energy. In order to ensure safe braking distance and improve energy recovery efficiency, the motor model and battery charging model were established, and the energy consumption function was formulated, moreover braking force plane was divided into four quadrants, and a minimum energy consumption braking torque distribution scheme based on STA second-order sliding mode controller (hereinafter referred to as STA-MECBTD) is proposed and the co-simulation of Simulink and Carsim is adopted. The results show that both the I-curve and the ECE regulations curve (hereinafter referred to as ECE-curve) can't balance the braking stability and energy recovery efficiency. The proposed scheme has a good comprehensive performance, which can quickly respond to driver demand and improve energy recovery efficiency.**

Index Terms* - *Electric vehicle, Brake torque distribution, I-curve, ECE regulations, STA

I. INTRODUCTION

According to statistics, vehicles frequently brake and start under urban driving conditions, in which the energy dissipated by the brakes accounts for 50% of the total driving energy[1], while the braking system of the traditional automobile converts the kinetic energy of the vehicle into mechanical friction braking. The heat energy is dissipated, resulting in a large amount of energy wastage and the vehicle is less energy efficient. Regenerative braking technology is a new technology to study how to recycle this part of kinetic energy to the vehicle energy storage system, which is of great significance for improving the energy efficiency of the vehicle and prolonging the driving range.

When the electric vehicle performs regenerative braking, the driver's braking feeling, the stability of the vehicle brake, and the energy recovery efficiency of the regenerative braking are important design goals[2] of the regenerative braking control strategy. In the research of regenerative braking control strategy, the braking force distribution strategy is the core of its research. In [3], the I-curve based force distribution strategy is adopted, which can effectively utilize the ground adhesion coefficient, and has a short braking distance, but the energy recovery is limited. In [4], Under the premise of considering the braking regulations and braking stability, a braking force distribution strategy is proposed according to the polyline consisting of horizontal axis, the ECE (Economic Commission of Europe) regulation line and the front wheel locking line, which can guarantee the braking regulations, and maximizes the recovery of regenerative energy, but because the distribution line is far from the ideal curve, it reduces the braking performance and braking stability of the car to some extent.[5] introduces a braking force distribution strategy with the lowest energy consumption, which focus on distribution, but there is no additional dynamic controller, and the maximum adhesion provided by the ground is not fully utilized. According to this strategy, when the vehicle is moving, the total braking force of the actual demand cannot be calculated. So the strategy doesn't have a real-time performance.

Under the conditions of ensuring braking safety and driver demand, this paper comprehensively considers the constraint mechanism of battery state and vehicle state, and studies how the electric vehicle braking process can recover energy to the greatest extent. The highlight of this paper is to design a Super-Twisting second-order sliding mode controller which responds quickly and sensitively to driver demand (braking strength) and can calculate driver demand braking force in real time under the maximum adhesion provided by the ground. Moreover, an energy consumption function is established to optimize online the distribution of electrical and hydraulic braking force. This paper uses Simulink and Carsim co-simulation, and the results show that the proposed strategy can meet the driver's braking requirements well, ensure the braking safety, have a short braking distance, and effectively improve the energy recovery efficiency. In short, it meets the driver demand, braking stability and energy recovery efficiency simultaneously, although which is difficult to meet at the same time before.

The rest of the paper is organized as follows: Section II introduces the layered controller architecture of the composite braking system; Section III presents the mathematical model of the composite braking system; Section IV analyzes the automotive braking dynamics; Section V formulates the braking force distribution strategy of the composite braking system; The simulation experiment was carried out in Section VI and compared with other schemes; Section VII draws the conclusions of this paper.

II. LAYERED CONTROLLER STRUCTURE

In this paper, a four-wheel-drive electric vehicle is taken as an example, and only the linear motion of the vehicle is considered, and the vehicle model adopts a two-dimensional model. The functions of the proposed layer controllers of the composite brake system are shown in Fig.1.

* This work is supported by National Key R&D Program of China under Grant 2018YFB0104803 and 2016YFB0100700.

978-1-7281-6321-5/19//$31.00 ©2019 IEEE

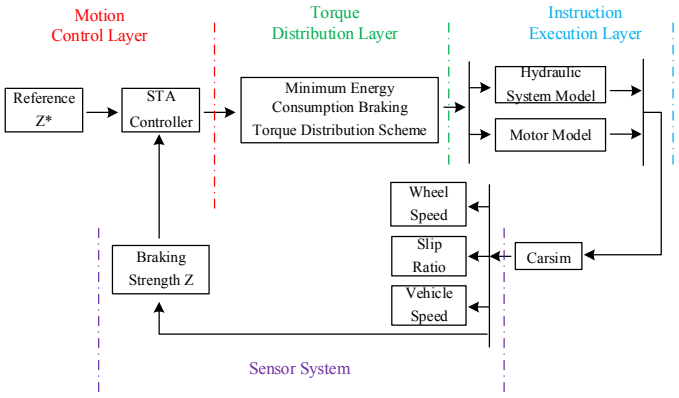

Fig.1. STA-MECBTD Control structure diagram.

1) Upper layer: Motion control layer. The driver demand (braking strength z) is taken as the control target, and the real-time total braking torque T_{sum} is calculated by the Super-Twisting second-order sliding mode algorithm;

2) Middle layer: Torque distribution layer. Under the premise of ensuring the safety of the brake, according to the expected total braking torque given by the upper layer, combined with the vehicle state driving information and the established allocation strategy, the total braking torque, electric braking torque and hydraulic braking torque of each wheel are calculated as expected.

3) Lower layer: Instruction execution layer. This layer contains the motor drive subsystem and the hydraulic brake subsystem. Combined with the distribution information of the middle layer, the electric mechanism power and hydraulic braking force command on each wheel are sent to the corresponding wheel subsystem to perform the work.

4) Sensor system: In this model, the motor torque X_m, the motor speed n_i and the vehicle centroid acceleration a are directly measured by the sensor. Relatively stable parameters are given in advance, namely the total mass M of the vehicle, the wheelbase L of the vehicle, the front wheelbase L_a, and the rear wheelbase L_b. The vehicle speed v is estimated using a Kalman filter.

III. Mathematical Model of Motor Regenerative Braking

A. Motor Model

Regenerative braking is a type of electrical braking that achieves energy recovery compared to reverse braking and energy consume braking, and is therefore also referred to as energy feedback braking[6]. According to the reversible working principle of motor and generator, when the electric vehicle regeneratively brakes, the motor generates the braking torque through the action of the controller, and converts the braking energy of the process into electric energy and stores it in the energy storage device such as the battery. The characteristics of the motor in the power generation state are basically the same as those in the driving state. When the motor speed is higher than the rated speed, the motor is braked at the rated power; when the motor speed is lower than the rated speed, the motor is braked at the rated torque. In addition, the driving state is differently, when the motor speed is very low, since the armature opposing electromotive force is too low, the regenerative braking effect basically disappears, and the braking torque generated by the regenerative braking is reduced to zero.

Thus, the motor braking torque model is

$$T=\begin{cases}9549.3P_n/n, & n\geq n_N\\ T_N, & n_L<n<n_N\\ 0, & n<n_L\end{cases} \tag{1}$$

Where T is the electrical braking torque, N*m; T_N is the rated torque of the motor, N*m; P_N is the rated power, kW; n is the motor speed, r/min; n_N is the rated motor speed, r/min; n_L is the regenerative braking failure speed, r/min.

B. Battery Model

The relationship between battery charging power and battery electromotive force, charging current and battery internal resistance is[7]

$$P_{ch}=(E_b-IR_b)I \tag{2}$$

Where, P_{ch} is the battery charging power, kW; E_b is the battery electromotive force, V; I is the charging current, A; R_b is the internal resistance of the battery, Ω. In order to protect the battery, the regenerative braking torque of the motor is limited by the maximum charging power and charging current allowed by the battery.

From the above analysis, the actual braking torque of the motor is determined by the motor torque characteristic and the battery charging power. The maximum braking torque is

$$T_{e\_\max}=\min\left\{\frac{P_{ch\_\max}}{\eta_{ch}\eta_{gen}w},T\right\} \tag{3}$$

Among them, P_{ch_max} is the maximum charging power of the battery, kw; η_{ch} is the charging efficiency, η_{gen} is the motor power generation efficiency; w is the motor angular velocity, rad/s.

IV. The Braking Dynamics of Vehicle

A. Ideal Braking Force Distribution Curve

The ideal braking force distribution curve[8] is the front and rear axle braking force distribution curve when the front and rear axles are locked at the same time during braking, which is also called the I-curve. Under this condition, the ground attachment conditions can be well utilized.

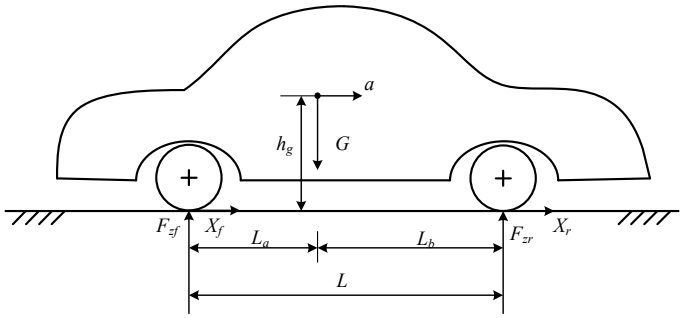

Fig.2. Braking force diagram of vehicle.

When vehicle brakes, it has a deceleration and corresponding braking strength $z = a/g$, and the load will shift. At this time, the front and rear axle loads are:

$$F_{zf} = \frac{G}{L}(L_b + z * h_g) \tag{4}$$

$$F_{zr} = \frac{G}{L}(L_a - z * h_g) \tag{5}$$

When the vehicle is locked, the total braking force:

$$X = \mu G = zG = X_f + X_r \tag{6}$$

The front and rear axle braking forces are:

$$X_f = \mu F_{zf} = \mu \frac{G}{L}(L_b + z * h_g) \tag{7}$$

$$X_r = \mu F_{zr} = \mu \frac{G}{L}(L_a - z * h_g) \tag{8}$$

From equations (1)-(5), the relationship between the braking force of the front and rear axles on the I-curve is

$$X_r = \frac{G}{2h_g}\sqrt{b^2 + \frac{4h_g L}{G}X_f} - X_f - \frac{Gb}{2h_g} \tag{9}$$

Where G is the vehicle gravity, N; X_f, X_r are the braking forces on the front and rear axles respectively, N; L, L_a, L_b are the vehicle wheelbase, front wheelbase, rear wheelbase, respectively, m; h_g is vehicle center of mass height, m.

B. ECE Brake Regulation Curve

The ECE brake regulations set clear requirements for the braking force of the front and rear axles of twin-axle vehicles. For the car, when the braking strength is z=0.2~0.8[9], the front axle utilized adhesion coefficient curve should be above the adhesion coefficient of the rear axle, and the utilized adhesion coefficient should satisfy $\mu \le (z + 0.07)/0.85$, so that the front wheel is first locked to ensure the stability of the vehicle braking direction. Therefore, under the ECE regulations, the front and rear axle braking forces are

$$\begin{cases} X_f = \dfrac{(z+0.07)}{0.85} * \dfrac{G}{L} * \left(L_b + zh_g\right) \\ X_r = G * z - X_f \\ \left(0.2 < z < 0.8\right) \end{cases} \tag{10}$$

From (6), $G * Z$ is the total braking force X, which is the sum of the front axle braking force X_f and the rear axle braking force X_r. As shown in the Fig.3, the curves z takes the value of 0.3, 0.4, 0.5, 0.6 respectively corresponding to are the relationship curves of the front and rear axles braking force in the case of different z or total braking force X. It can be seen that when the total braking force of the demand is constant, for instance, z takes 0.3, the $z = 0.3$ curve intersects the I-curve and ECE-curve at point A and B respectively. According to the I- curve distribution, the front axle braking force (reference to point A) is small, and the front and rear axle braking forces are not much different; according to the ECE-curve distribution, the front axle braking force is fully excavated (reference to point B), and front wheels have a high adhesion utilization rate to the ground. In general, the front and rear axle braking force distribution should be within the I-curve and ECE-curve, and I-curve and ECE-curve the are the lower and upper boundaries (Hereinafter referred to as LB and UB) of the front axle braking force X_f respectively.

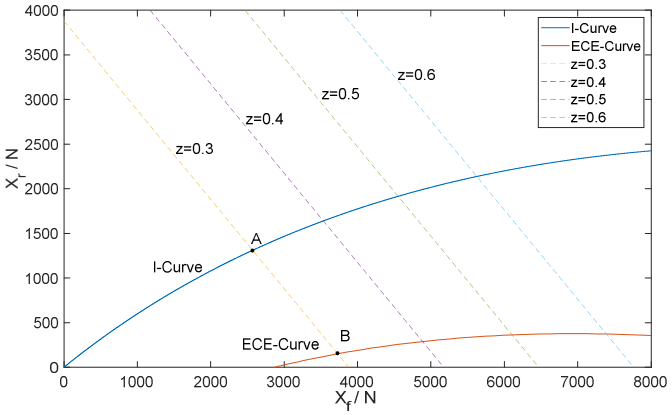

Fig.3. I-curve and ECE-curve.

C. Objective Function for Minimum Small Braking Losses

Electric vehicles not only have a regenerative braking system, but also a hydraulic braking system, that is, an electro-mechanical composite braking system. In order to achieve the dual goals of energy recovery and stable braking performance, the electrical and hydraulic braking force must be properly distributed. In this paper, a minimum braking loss strategy for electro-hydraulic braking torque distribution is used. Under the premise of meeting the ECE regulations, the minimum braking loss is the target, and the braking stability requirements are taken into account to maximize the recovery of energy and redistribute the front and rear axle braking force and electro-hydraulic braking force.

1) the objective function. For four-wheel-drive electric vehicles, if the irreversible dissipation of rolling and windage is not considered, the total power loss P_{loss} can be expressed as

$$P_{loss} = P_{loss,mech} + P_{loss,slip} + P_{loss,hydra} \tag{11}$$

Among them, $P_{loss,slip}$ represents the sum of longitudinal slip loss and lateral slip loss. Since this paper only considers the longitudinal problem of the vehicle, the car is traveling in a straight line, so its side slip loss is negligible. The total slip loss can be expressed as the ratio of the longitudinal force to the tire stiffness.

$$P_{loss,slip} \approx \frac{X_i^2 V}{K_i} = \frac{X_i^2 V}{DF_{zi}} \tag{12}$$

Where, X_i (i = 1, 2, 3, 4) refers to the braking force on each wheel; V represents the vehicle speed; K_i (i = 1, 2, 3, 4) refers to the stiffness of each wheel, D is the stiffness of the wheel, and F_{zi}(i = 1, 2, 3, 4) is the load on each wheel.

$P_{loss,hydro}$ is the hydraulic braking loss, which is completely dissipated as thermal energy.

$$P_{loss,hydra} = (1 - j_i) X_i n_i r / 9.55 \tag{13}$$

Where j_i(i=1,2,3,4) refers to the ratio of the electric braking force on each wheel to the total braking force on the wheel; r is the effective radius of rotation of the wheel.

$P_{loss,mech}$ is the sum of motor loss and transmission loss, and its expression is

$$P_{loss,mech} = n_i j_i X_i r(1 - \eta_i(n_i, j_i, X_i)) / 9.55 \tag{14}$$

Where η_i is the average efficiency of electromechanical transmission and n_i is the wheel speed.

Thus, the objective function is defined as the minimum of the total loss, expressed as

$$J = \min \sum (n_i j_i X_i r(1-\eta_i(n_i, j_i, X_i))/9.55 + \frac{X_i^2 V}{K_i} + (1-j_i) X_i n_i r/9.55) \quad (15)$$

2) Simplify the objective function

The regenerative power is mainly affected by the motor speed, the longitudinal load of the wheel, and the electrical mechanism dynamics. The influence of the change of the speed and vertical load is much lower than the influence of the braking force. The regenerative power differential relationship can be expressed as

$$\begin{aligned} \frac{dP_{gen,f/r}}{dX_{f/r}} &= \frac{\partial P_{gen,f/r}}{\partial n_{f/r}} \frac{dn_{f/r}}{dX_{f/r}} + \frac{\partial P_{gen,f/r}}{\partial F_{zf/r}} \frac{dF_{zf/r}}{dX_{f/r}} + \frac{\partial P_{gen,f/r}}{dX_{f/r}} \\ &= o(\frac{\partial P_{gen,f/r}}{dX_{f/r}}) + \frac{\partial P_{gen,f/r}}{dX_{f/r}} \\ &\approx \frac{\partial P_{gen,f/r}}{dX_{f/r}} \end{aligned} \quad (16)$$

Where $o(\bullet)$ means that the item is small compared to the brackets and can be ignored.

If the braking force on the wheel is determined, the maximum value of the electric braking force X_m should be selected to obtain a higher regenerative power, which is

$$j_i = \min\left(\frac{T_{e\_\max}}{rX_i}, 1\right) \quad (17)$$

This equation shows that when the motor can provide the required braking torque for the wheel, all of the torque will be provided by the motor and will not increase the hydraulic force. On the other hand, when the required braking torque exceeds the maximum torque provided, the motor outputs its maximum torque.

V. Braking Force Distribution Strategy

A. Super-Twisting Second-Order Sliding Mode Control Law

The concrete expression of the second-order sliding mode STA can be written as[10]:

$$u = \lambda |s|^{1/2} sign(s) + \int \alpha sign(s) dt \quad (18)$$

Where s is a sliding mode variable and the control parameters λ>0, α>0.

According to the literature [11], the sliding mode proportional term ks is introduced in the second-order sliding mode STA, which does not affect the stability of the system. As long as the k, ks is properly set, the sliding mode variable gain of the system away from the equilibrium point can be increased. Moreover, it can increase control command output, ensure robustness, and improve convergence speed. When reaching the equilibrium point, STA plays a leading role to ensure the stability and robustness of the system in the equilibrium point neighborhood.

In this paper, the braking strength z of the driver demand is taken as the control target, and the sliding surface is designed as

$$s = z^* - z \quad (19)$$

The second-order sliding mode STA control law is

$$T_{sum} = u = \lambda |s|^{1/2} sign(s) + \int \alpha sign(s) dt + ks \quad (20)$$

When the vehicle brakes, the vehicle deceleration a can be read from the vehicle's centroid acceleration sensor, and then the actual braking strength z of the vehicle is obtained, According to the second-order sliding mode STA control law, the driver's braking demand is quickly and sensitively responded , and real time calculate the total braking torque T_{sum} of the vehicle demand.

B. Brake Force Distribution Scheme

It should be pointed out that the relationship between braking force in electric vehicles is:

Total braking force X = front axle braking force X_f + rear axle braking force X_r;

Front axle braking force X_f= front axle electric braking force X_{m_f} + front axle hydraulic braking force X_{h_f};

Rear axle braking force X_r = rear axle electric braking force X_{m_r} + rear axle hydraulic braking force X_{h_r}.

According to the relationship between the different front and rear axle braking forces X_f, X_r, and the electric braking force X_m, the braking force decision plane can be divided into four quadrants.

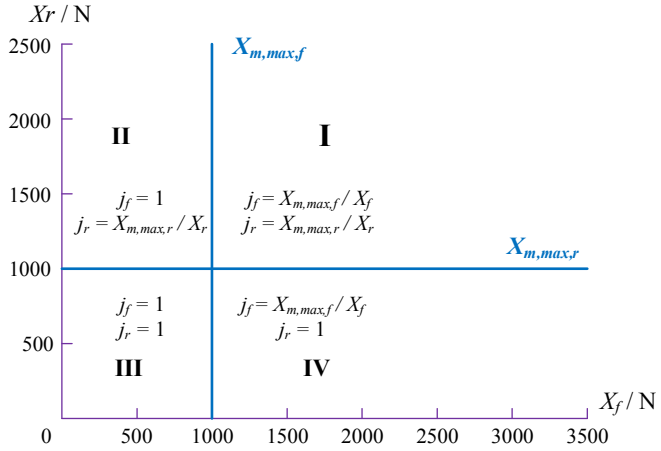

Fig.4. Four quadrant diagram of braking force.

Where LB is given by equation (7) and UB is given by equation (10). According to the previous analysis, the front axle braking force X_f of the vehicle should be within LB and UB, that is,

$$\mathrm{LB} \le X_f \le \mathrm{UB} \quad (21)$$

In addition, the braking force of each wheel should not exceed the maximum static friction provided by the road surface.

$$X_i \le \mu_{\max} F_{zi} \quad (22)$$

In this paper, the maximum static friction coefficient of the road surface is set as $\mu_{\max} = 0.85$.

In Fig.4:

1) If the feasible area contains only quadrant II, that is, the maximum electric braking force $X_{m,max,f}$ the front wheel providing is larger than UB, while the maximum electric

braking force $X_{m,max,r}$ of the rear wheel is smaller than the vehicle's total demand force X minus UB. At this time, the required braking force X_f of the front axle should be set to UB, and the required braking force of the front axle is all provided by the front axle electric braking force; The braking force X_r of the rear axle demand is set to the difference between the total braking force X and the UB, the rear axle electric braking force X_{m_r} takes $X_{m,max,r}$, and the remaining portion is provided by the rear axle hydraulic braking force X_{h_r};

2) If the feasible area contains only quadrant IV, that is, the maximum electric braking force $X_{m,max,f}$ the front wheel providing is smaller than LB, while the maximum electric braking force $X_{m,max,r}$ of the rear wheel is larger than the vehicle's total demand force X minus LB, At this time, the required braking force X_f of the front axle should be set to LB, the front axle electric braking force X_{m_f} should be $X_{m,max,f}$, and the remaining part should be provided by the front axle hydraulic braking force X_{h_f}; The required braking force X_r is all provided by the rear axle electrical braking force.

3) If the feasible area contains quadrants I or III, then the search algorithm is used to search for optimization. In quadrants I and III, the optimization is slightly different: in quadrant I, the electric braking force is set at its maximum value, and in quadrant III, the hydraulic pressure is set to zero. Finally, the optimal distribution of the braking force can be determined. In this process, the optimization algorithm is the classic Newton method. The initial value is set to half the braking force of the reference value. The iteration will continue unless the error of two adjacent values is within tolerance.

Table I
Electric vehicle parameters

Total vehicle quality M/kg	1320	Motor rated power P_N/kW	15
Wheelbase L/m	2.6	Motor rated torque T_N/N*m	220
Front wheelbase L_a/m	1.04	Motor rated speed n_N/r*min^{-1}	800
Rear wheelbase L_b/m	1.56	Regenerative power failure speed n_L/r*min^{-1}	20
Centroid height h_g/m	0.54	Battery maximum charging power P_{ch_max}/kW	65
Wheel radius r/m	0.27	Motor efficiency	0.9
Moment of inertia J/ kg*m^2	37.6		
Stiffness coefficient D	20		

The steps for optimizing the electrohydraulic braking force distribution are as follows:

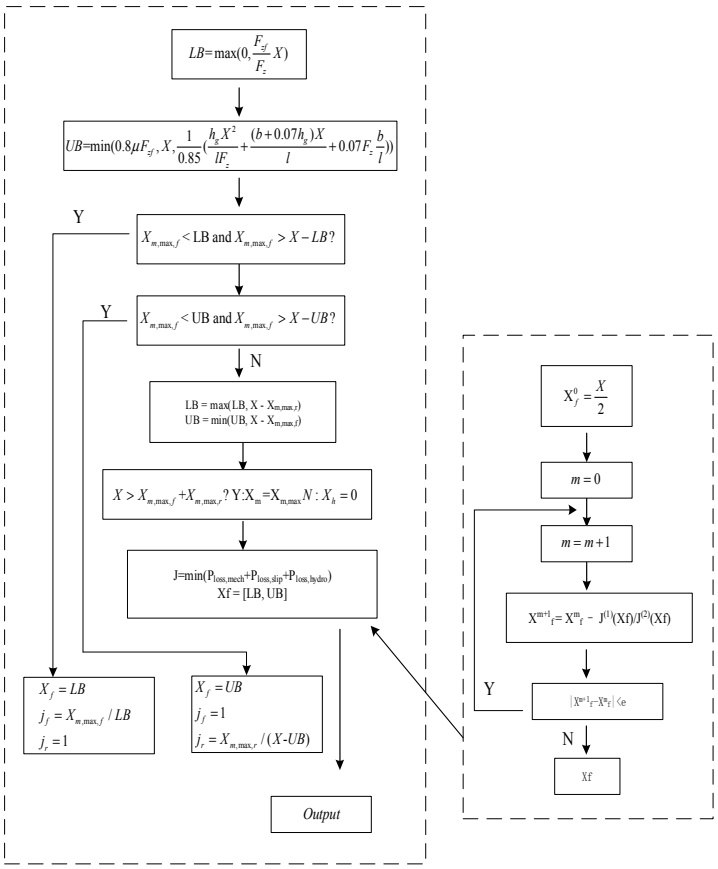

Fig.5. Braking force distribution flow chart.

VI. Simulation Analysis

Electric vehicle parameters are shown in Table I. Simulation conditions: a single homogeneous road surface with an adhesion coefficient of 0.85, an initial speed of the vehicle speed of 100 km/h, and braking with a braking strength of z=0.5.

Table II
Energy recovery and braking distance for different control strategies

Control Strategy	Brake total energy /kJ	Recycling brake energy /kJ	Energy recovery rate	Braking distance /m
I-curve	509.259	181.36	35.61%	92.14
ECE-curve	509.259	172.13	33.80%	106
STA-MECBTD	509.259	196.61	38.61%	80.37

It can be seen from the data in Table II that when braking according to the torque distribution strategy of the ECE-curve, the braking distance is the longest, and the recovered energy is also the least, which is 172.13kJ, accounting for 33.80% of the total braking energy. This is because for the four-wheel drive vehicle, both the front and rear wheels have a regenerative braking function. If The ECE-curve is adopted, the front wheel braking force reaches the upper limit, and the front wheel tire loss will be more serious. Simultaneously the rear wheel braking force distributed is very little, then the total energy recovered will be reduced; when braking according to the torque distribution strategy of the I-curve, the braking distance is shorter, and the recovered energy is more, which is 181.36kJ, accounting for 35.61% of the total braking energy.

When the I-curve braking strategy is adopted, the front and rear wheel braking force distribution is relatively uniform, and the front and rear wheels are on the verge of being locked. Therefore, the overall braking force is large, the braking distance is short, and the front and rear wheels are all energy-recovered, and the energy recovered is also more; when braking according to the STA-MECBTD, the braking distance is the shortest, and the most recovered energy is 196.61 kJ, accounting for 38.61% of the total braking energy. Overall, the STA-MECBTD can recover as much of the braking energy as possible while satisfying the safety of the brake.

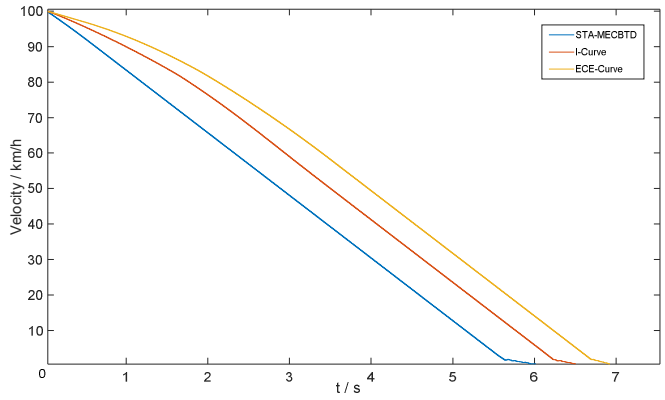

Fig.6. Vehicle speed simulation curve.

From the longitudinal speed of the vehicle, Fig.6 shows the braking time of the I-curve braking strategy is short, around 6.5s, and the vehicle deceleration is not uniform enough; the braking time of the ECE-curve braking strategy is the longest, around 7s, and the vehicle deceleration is the most uneven. STA-MECBTD can provide the most stable braking feeling under the premise of satisfying driver's braking demand, and the vehicle speed is evenly decelerated. From 100km/h to stop, the braking time is the shortest, about 6s. Overall, the STA-MECBTD has the shortest braking time and the most stable braking performance.

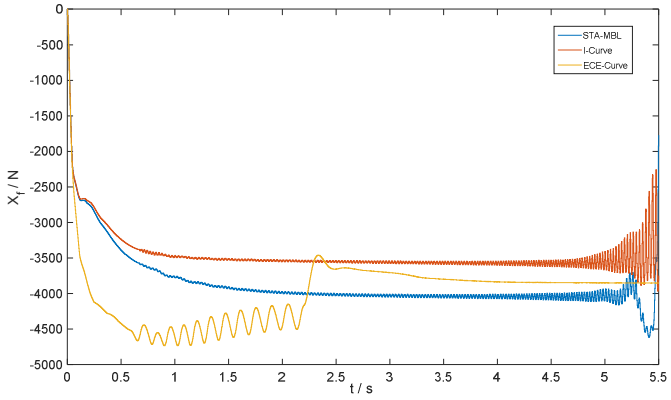

Fig7. Front axle braking torque distribution curve.

From the three schemes for the front axle braking force distributed by the car (excluding the vicinity of the parking time), the I-curve braking strategy can distribute a relatively stable braking force for the front axle, but the braking force is a little small; The front axle braking force distributed by the ECE-curve braking strategy fluctuates greatly and is unstable, which also explains the reason for its poor braking effect. The STA-MECBTD not only provides a relatively stable braking force, but also distributes more braking force than the I-curve, which is why it can recover more braking energy. Overall, the STA-MECBTD has the best braking force distribution effect.

VII. Conclusion and Outlook

The braking force distribution scheme can greatly affect the braking energy recovery efficiency[12]. Based on the considerations of vehicle braking stability, motor characteristics, battery characteristics and driver demand, this paper proposes a STA-MECBTD, which greatly recovers the regenerative braking energy.

The three schemes of I-curve braking force distribution, ECE-curve braking force distribution and STA-MECBTD are compared and analyzed. The results show that the proposed scheme can quickly respond to the driver's demand and make full use of motor regenerative braking, simultaneously recover more braking energy.

The future research directions should focus on real-time use of the maximum adhesion provided by the ground, as well as a faster and more stable controller to satisfy the driver's braking needs sensitively and accurately, and to achieve shorter braking distances and recover more braking energy.

Acknowledgment

This work is supported by National Key R&D Program of China under Grant 2018YFB0104803 and 2016YFB0100700.

References

[1] Walker A M, Lamperthm U, Wilkins S. On friction braking demand with regenerative braking[R]. SAE 2002-01-2581, 2002

[2] Cikanek S R, Baileyk E. RegenerativeBrakingSystem fora hybrid electric vehicle[c]//Proceedings of the American Control Conference. [s.1.]:IEEE,2002: 3129—3134

[3] X. Nian, F. Peng, and H. Zhang, "Regenerative braking system of electric vehicle driven by brushless DC motor," IEEE Trans. Ind. Electron. vol. 61,no. 10, pp. 5798–5808, Oct. 2014.

[4] LI Peng, JIN Dafeng, LUO Yugong. Regenerative braking control strategy for a mild HEV[J] .Automotive Engineering, 2005, 27(5):570-574.

[5] Huizhong Sun, Hui Wang, and Xinchen Zhao. Line Braking Torque Allocation Scheme for Minimal Braking Loss of Four-Wheel-Drive Electric Vehicles. IEEE Transactions on Vehicular Technology, vol.68,no. 1, Jan 2019.

[6] Gong Daoqing. Research on electric brake composite control system of four-wheel independent drive hub motor[D].Hunan University,2018.

[7] Liu Lijun, Ji Fenzhu, Yang Shi chun, Xu Bin. Electromechanical composite brake control strategy based on ECE regulations and I-curve [J]. Journal of Beijing University of Aeronautics and Astronautics, 2013,39(01):138-142.

[8] Yu Zhisheng. Optimal design of braking force distribution in axis for car[M]. Beijing：China Machine Press，1999：21—24(in Chinese).

[9] Shu Hong, Wu Jiansheng. Optimal design of braking force distribution in axis for ear[J]. Automobile Research＆Development, 1999, 2(2): 23-25, 3l(in Chinese).

[10] Levant A. Sliding Order and Sliding Accuracy in Sliding Mode Control[J]. International Journal of Control, 1993, 58(6): 1247-1263.

[11] Zhang Qinchao, Ma Ruiqing, HuangFu Yiqiu, Wang Jiao. Design and Research of Second-Order Sliding Mode Control Law for Super-Twisting Algorithm of Motor Speed Link[J].Journal of Northwestern Polytechnical University,2016,34(04):669-676.

[12] K. Itani, A. De Bernardinis, K. Zoubir, A. Jammal, and M. Oueidat, "Regenerative braking modeling, control, and simulation of a hybrid energy storage system for an electric vehicle in extreme conditions," IEEE Trans.Transp. Electrific, vol.2, no.4, pp. 465–479, Dec.2016.